THE ASTROPHYSICAL JOURNAL, 206:128–137, 1976 May 15

THE STRUCTURE AND MASS FUNCTION OF THE GLOBULAR CLUSTER M3

G. S. DA COSTA AND K. C. FREEMAN
Mount Stromlo and Siding Spring Observatory, Research School of Physical Sciences,
Australian National University
Received 1975 September 8

ABSTRACT

A detailed dynamical model of the globular cluster M3 is presented. The model is tidally limited and includes a realistic distribution of stellar masses. It is used to derive a *total* luminosity function for the cluster from the published luminosity function, and to give estimates of its total mass ($[3.30 \pm 0.15] \times 10^5\ M_\odot$) and M/L_V ratio (1.6 ± 0.2 solar units). The model gives an excellent fit to the observed radial distribution of surface brightness and star counts over five decades in surface brightness: a good fit is not possible with the corresponding single-mass models.

Subject headings: clusters: globular — stars: stellar dynamics

I. INTRODUCTION

The radial distributions of surface brightness and star number density are now available for many globular clusters. Most of these observed profiles extend over three to four decades of surface brightness, and most can be well represented by King's (1966*a*) dynamical cluster models (Peterson and King 1975): in these models all stars have the same mass, and the velocity distribution has the "lowered Gaussian" form of equation (1). For a few clusters, however (including 47 Tuc [Illingworth 1973], M3 [this paper] and M15 [Newell, Norris, and Da Costa, in preparation]), the observed surface brightness profiles cover five or more decades, and in each case the observed profile deviates significantly from the best-fit single-mass model (see Fig. 1).

We have constructed globular cluster models which include a realistic mass spectrum. In a globular cluster the giants contribute almost all the visible light, while the low-mass stars dominate the gravitational field in which these giants move. If we know the bright end of the luminosity function, and the radial surface brightness distribution, we can use these dynamical models in an iterative procedure to derive a self-consistent picture of the cluster's dynamical structure and its mass (or luminosity) function. As part of a continuing program on the structure of globular clusters, we investigate in this paper the structure and mass function of the globular cluster M3, using as initial data Sandage's (1954, 1957) luminosity function and an electronographic surface brightness profile generously provided by Dr. G. E. Kron and Dr. A. V. Hewitt, combined with star counts from King *et al.* (1968). Our main purpose is to show how a dynamical model, with the usual lowered Gaussian distribution function and a mass spectrum based on the observed luminosity function, gives an excellent representation of this cluster's surface brightness profile.

II. THE MODELS

In a classic paper, King (1966*a*) described a one-parameter set of dynamical models for spherical star clusters, based on steady-state solutions of the Fokker-Planck equation. These models are spatially limited by the tidal field of our Galaxy, have an isotropic velocity distribution, and contain the further assumption that the stars all have the same mass. In this section we present the theory for a set of models in which this last assumption is relaxed.

The relaxation time at the center of a globular cluster is a small fraction of its age (see, for example, Peterson and King 1975), so stellar encounters will have strongly affected the form of the velocity distribution function there, driving it toward a Maxwellian distribution. However, because the galactic tidal field acts spatially to limit the cluster, the velocity distribution function becomes zero at the velocity needed to reach the cluster boundary, rather than at the value for escape to infinity. These effects are described by the steady-state solutions of the Fokker-Planck equation subject to a finite velocity cutoff, and the lowered Gaussian velocity distribution used by King (1966*a*) is an analytic approximation (Michie 1963; King 1965) to these solutions. We write this distribution function in terms of the energy E since, according to Jeans's theorem, the distribution function must then be the same function of E at all points in phase space.

We assume that the stars of the cluster can be grouped into a number of *mass classes*, each characterized by a mass m_i, and that the number density in phase space for each mass class is given by the distribution function (*cf.* King 1966*a*)

$$f_i(r, v) = \alpha_i\left[\exp\left(-\frac{E_i}{m_i\sigma_i^2}\right) - \exp\left(\frac{C}{\sigma_i^2}\right)\right], \quad E_i \le -m_i C; \quad (1)$$

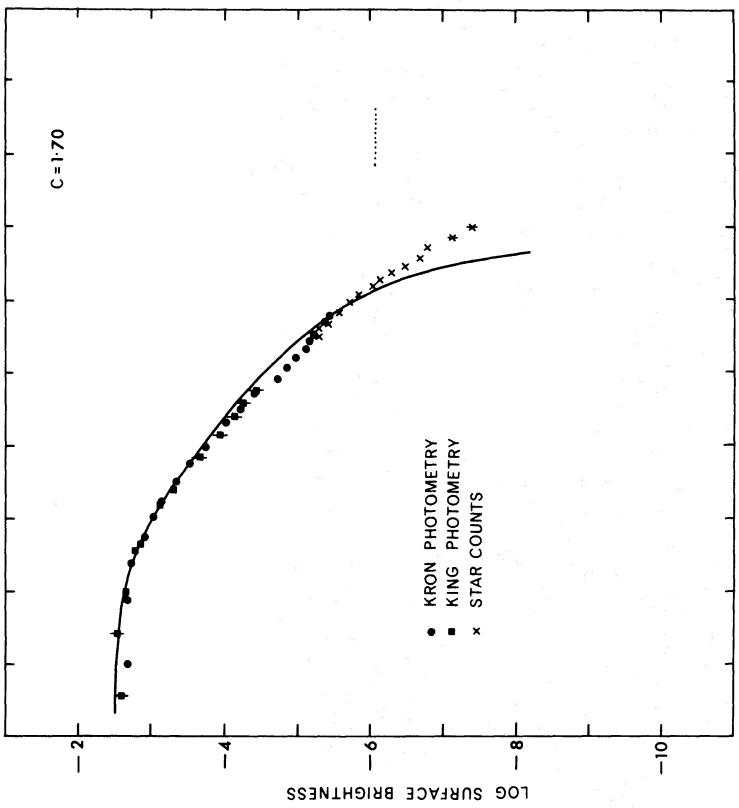

FIG. 1b

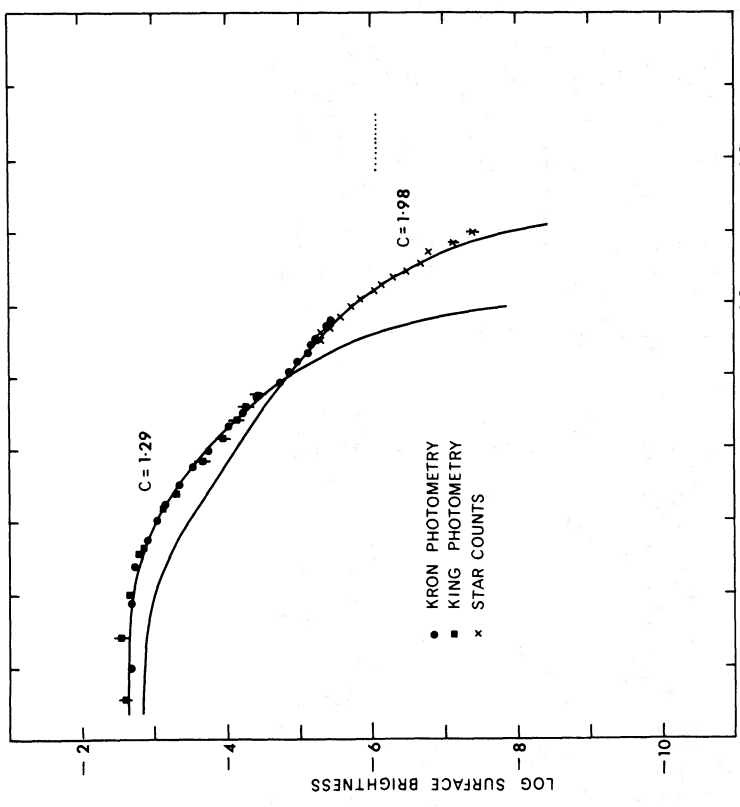

FIG. 1a

FIG. 1.—Comparison of the observed surface brightness profile for M3 with the surface density distribution of single-mass-class models. Curves are chosen (*a*) to fit best the inner and outer parts of the observed profile, (*b*) to fit best the entire profile. The curves are labeled with parameter $c = \log r_t/r_c$ and the surface brightness unit is number of 10.00V mag stars per arcsec^2.

here r and v are (spherical) radius and velocity, α_i and σ_i^2 are positive constants related to the number and velocity dispersion of stars in this mass class, and $C > 0$ is a constant. The energy E_i for stars of this mass class is given by

$$E_i = \tfrac{1}{2}m_i v^2 + m_i\psi(r)\,, \tag{2}$$

where $\psi(r)$ is the smoothed gravitational potential for the cluster. The boundary of the cluster is given implicitly by the equation

$$\psi(r_t) + C = 0\,, \tag{3}$$

and is the same for each mass class, as required by the tidal cutoff (King 1962). The total distribution function at each point is then the sum of the components for each mass class. The density ρ_i of each mass class at any point can now be found by integrating the distribution function $f_i(r, v)$ over velocity,

$$\rho_i(\psi) = \int_{E_i \leqslant -m_i C} m_i f_i(r, v) 4\pi v^2 dv\,; \tag{4}$$

and the problem is reduced to finding a solution to the (nonlinear) Poisson equation

$$\nabla^2\psi = 4\pi G\Sigma_i\rho_i(r, \psi)\,, \tag{5}$$

subject to the boundary conditions $\psi = -A(A > 0)$ at $r = 0$ and $\psi = -C$ at $r = r_t$, the as yet undetermined boundary of the cluster.

We now make the assumption that there is full *equipartition of energy*, so

$$m_i\sigma_i^2 = m_j\sigma_j^2\,. \tag{6}$$

We then transform to dimensionless variables. Write $U = \psi + C$, $r = r'r_t$, $m_i = m_i'm_1$, $U = U'\sigma_1^2$, $C = C'\sigma_1^2$, $\alpha_i = \alpha_i'\alpha_1$, $\rho_i = \rho_i'\alpha_1 m_1\sigma_1^3$, and

$$a_i = \alpha_i' \exp\left[-C'(1 - m_i')\right].$$

Integrating equation (4) gives the dimensionless density for the ith mass class as

$$\begin{aligned}\rho_i(U) = {} & a_i m_i^{-1/2} \exp(C) \\ & \times \left[(2\pi)^{3/2} \exp(-m_i U) \operatorname{erf}(-m_i U)^{1/2}\right. \\ & \left. - 2^{5/2}\pi(-m_i U)^{1/2} - 2^{7/2}\pi(-m_i U)^{3/2}/3\right],\end{aligned} \tag{7}$$

where we have suppressed the primes. Poisson's equation becomes

$$r^{-2}\frac{d}{dr}\left(r^2\frac{dU}{dr}\right) = \lambda\Sigma\rho_i(U)\,, \tag{8}$$

with the boundary conditions $U(0) = -D(D > 0)$ and $U(1) = 0$. The number $\lambda = 4\pi G r_t^2\sigma_1\alpha_1 m_1 \exp(C)$ behaves as an eigenvalue because the maximum radius r_t, which we have chosen as the radial scaling factor, and the dimensionless cutoff energy C, must be determined at the same time as $U(r)$ (*cf.* Prendergast and Tomer 1970; Wilson 1975).

Equation (8) is solved numerically on a grid of 51 radial points $0 \leq x_k \leq 1$. The central dimensionless potential D, the relative masses m_i, and the relative number factors α_i serve over a large range of values to specify a unique solution. For a given set $\{m_i, \alpha_i\}$, increasing D (i.e., deepening the central potential well) increases the central concentration of the mass class containing the most massive stars (always mass class 1), while for fixed D and m_i, increasing the $\{\alpha_i\}$ values also increases this central concentration. The central concentration of a model is measured by the parameter β_1, which is the ratio of the tidal radius to the core radius for mass class 1. This core radius $r_{c,1}$ is defined by $4\pi G r_{c,1}\Sigma\rho_i(-D) = 9\sigma_1^2$; cf. King (1966*a*). The central concentration of each mass class is defined similarly. The number factors α_i determine for each mass class the *relative total mass* μ_i, where

$$\mu_i = \int_0^1 \rho_i(r) 4\pi r^2 dr \Big/ \int_0^1 \rho_1(r) 4\pi r^2 dr\,; \tag{9}$$

μ_i is the ratio of the total mass in the ith mass class to the total mass in mass class 1. The variation of μ_i with mass class leads to the mass function of the model.

A model for a particular cluster is constructed by varying the number factors $\{\alpha_i\}$ and the central potential D iteratively until the concentration parameter β_1 and the relative total masses $\{\mu_i\}$ equal the values consistent with the data. A first approximation to the required value of β_1 comes from fitting a single mass class model to the star counts in the outer regions of the particular cluster. The output of the model is then the run of dimensionless space density with dimensionless radius for each mass class.

We have two numerical checks on our procedure. (i) Our models with a single mass class are indistinguishable from those of King (1966*a*). (ii) The virial theorem is satisfied for all models considered here, to better than 0.01 percent of the dimensionless kinetic energy.

To compare the model with observations, the space densities are first projected to give surface densities. Each mass class is then given a mean magnitude for stars of its mass, and the total surface brightness at each radius point calculated, allowing for the fact that not all the stars in each mass class contribute to the light output; some are white dwarfs (see §III). The fraction of horizontal-branch stars in each mass class must also be specified, along with the horizontal-branch magnitude. For completeness a mean white-dwarf magnitude is also specified. The output from this routine is then a plot of log (normalized surface brightness) against log (radius/$r_{c,1}$), a parameter which is a measure of the integrated apparent magnitude, and the M/L value (in solar units) for this model. Since it is a dimensionless number, the M/L value of the model can be compared directly to the M/L values of real clusters: this provides an instant check on the usefulness of the model. The model surface brightness profile is then compared to the observed profile; provided the fit is satisfactory, the intercepts on the axes in the log (surface brightness) $-$ log r plane

determine the central surface brightness and the tidal radius. Once these scale factors are known, the dimensionless model parameters can be converted into dimensional quantities. In particular, we have the following conversion formulae.

a) Mass of cluster:

$$M(M_\odot) = 18\xi r_t \langle v_1^2 \rangle_{0,r} , \qquad (10)$$

where r_t is the tidal radius in parsecs, $(\langle v_1^2 \rangle_{0,r})^{1/2}$ is the central velocity dispersion (in km s^{-1}) along the line of sight of the stars of mass class 1, and ξ is the dimensionless mass of the cluster given by $\xi = \lambda \int_0^1 \Sigma_i \rho_i(r) 4\pi r^2 dr$.

b) Central density:

$$d_0(M_\odot \text{ pc}^{-3}) = 18\delta \frac{\langle v_1^2 \rangle_{0,r}}{r_t^2} , \qquad (11)$$

where $\delta = \lambda \Sigma_i \rho_i(r = 0)$ is the dimensionless central density.

c) Escape velocity from center of cluster:

$$(v_e)_0 = (2D \langle v_1^2 \rangle_{0,r})^{1/2} , \qquad (12)$$

where D is the dimensionless central potential.

Now we discuss the construction of a model for the cluster M3.

III. MODEL FOR M3

Figure 1 shows the surface brightness profile for M3 (NGC 5272): this profile comes from photoelectric photometry by King (1966*b*), electronographic photometry by Kron and Hewitt (unpublished), and star counts by King *et al.* (1968). The curves in Figure 1*a* are single-mass models (labeled with their value of $c = \log r_t/r_c$), chosen independently to fit best the inner and outer parts of the profile. In Figure 1*b*, the curve is the single-mass model which gives the best eye fit to the profile over the whole five decades of surface brightness data. It seems clear that an adequate representation is not possible with a single-mass model of this family, which provides the motivation to construct a more realistic model for this particular cluster.

First we need to adopt a mass function for M3. Sandage's (1954, 1957) observed luminosity function for the inner part of the cluster was extended to fainter magnitudes by fitting to it the normalized solar neighborhood luminosity function from Wielen (1973). This complete luminosity function was then split into 10 groups: groups 1 and 2 contain all stars above the main-sequence turnoff, groups 3 and 4 are the remainder of the Sandage luminosity function, and groups 5 to 10 are the extension (see Fig. 2). For each group the mean M_V was calculated, and a representative mass assigned as follows.

From the results of Simoda and Iben (1970), Iben (1971), Copeland, Jensen, and Jørgensen (1970), McCluskey and Kondo (1972), and Harris, Strand, and Worley (1963), an M_{bol}(mass) relation was derived for various stellar ages, assuming the He abundance $Y = 0.30$ and the metal abundance $\log Z = -3.3$ (Sandage 1970). The adopted age was 10×10^9 years, which gives the giant mass as 0.83 $M_\odot$. Masses were then assigned to the main-sequence groups using bolometric corrections derived from a mean relation constructed from the data of Johnson (1966), Harris (1963), Vardya (1970), and Greenstein, Neugebauer, and Becklin (1971). We could then calculate the relative total mass for the "visible" stars of each mass class from the number of stars in each class; before proceeding, however, there are two comments. (i) These relative total masses do not include the mass

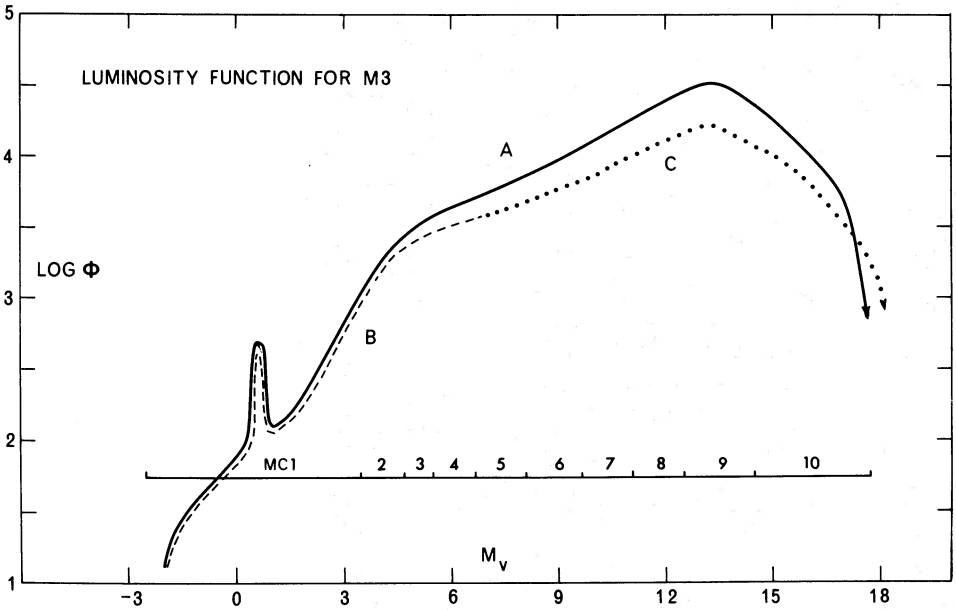

FIG. 2.—Luminosity function for M3. Φ is the number of stars between $M_V - 0.1$ and $M_V + 0.1$. Curve A is for the entire cluster, curve B is the Sandage function, and curve C is the extension of B based on the normalized solar-neighborhood luminosity function. The 10 mass classes are also shown.

distribution of the white dwarfs in the cluster. (ii) The adopted luminosity function pertains to a circular region of radius 8′ centered on the cluster's nucleus, so it underestimates the relative number of lower mass stars, which are less centrally concentrated than the more massive giants. We must include these two points through an iterative procedure in the model construction.

The number of white dwarfs was estimated by fitting the Salpeter (1955) initial luminosity function as modified by Sandage (1957) below the turnoff point and assuming that all stars more massive than the current giant mass have become white dwarfs. The mean white-dwarf mass was taken to be 0.6 $M_\odot$ (Wickramasinghe and Strittmatter 1971; see also Trimble and Greenstein 1972; Shipman 1972): for the first iteration we assumed that they were uniformly distributed between 0.83 $M_\odot$ and 0.4 $M_\odot$. The upper limit was chosen for computational convenience (0.83 $M_\odot$ is the mass for the most massive class 1); from the references above, however, it is seen to be a realistic upper limit because there are few more massive white dwarfs. At the lower limit, the number of main-sequence stars of this mass is already so much larger than the number of white dwarfs that the white dwarfs do not contribute significantly to this mass class. To construct the first model, the relative total masses derived from the Sandage/solar neighborhood luminosity function were adjusted for this uniform white-dwarf distribution. This model (*model A*) already fits the luminosity profile significantly better than the model of Figure 1*b*.

The relative total masses $\mu_i(A)$ for the lower mass classes in model A are too small because they are based on the adopted luminosity function, which holds only for the region $r < 8' \approx 0.2r_t$ (for all models, comparison with the observed luminosity profile gave $r_t \approx 40'$). To correct this deficiency, we calculated from model A the fraction $f_i(A)$ of each mass class within $0.2r_t$. From these fractions, we then chose the relative total masses μ_i(B) for the next model (*model B*) so that its population within the region $r < 0.2r_t$ conforms to the mass function μ_i(LF) derived from the adopted luminosity function and the associated uniform distribution of white dwarfs, i.e.,

$$\mu_i(\mathrm{B}) = \mu_i(\mathrm{LF})/f_i(\mathrm{A}) . \quad (13)$$

This procedure was repeated once to construct model C:

$$\mu_i(\mathrm{C}) = \mu_i(\mathrm{LF})/f_i(\mathrm{B}) . \quad (14)$$

The relative total masses μ_i(B), μ_i(C) did not differ significantly.

At this stage we have a dynamical model for which $\{\mu_i\}$ is known and which has a uniform distribution of white dwarfs between 0.83 $M_\odot$ and 0.4 $M_\odot$. We do not yet know what fraction of each mass class consists of white dwarfs; to estimate these fractions, we now vary white dwarf distribution subject to these constraints:

(*a*) The surface brightness profile calculated from the model fits the observed profile.

(*b*) Let N_i be the number of stars in the ith mass class from Sandage's luminosity function, n_i be the number of stars within $0.2r_t$ calculated from the model, and x_i the fraction of white dwarfs in this mass class. We want to find a set of fractions x_i such that $(1 - x_i)n_i/N_i$ has the same value (within about 1%) for each mass class, with the constraints that the total number of white dwarfs is fixed and that their average mass is 0.6 $M_\odot$; i.e., $\Sigma x_i n_i/\Sigma n_i = 0.088$ (0.088 of the total number of stars are white dwarfs) and $\Sigma x_i n_i m_i/\Sigma x_i n_i = 0.6\ M_\odot$.

(*c*) The model M/L ratio agrees with the M/L calculated from the mass of the cluster (derived from the luminosity function) and the total luminosity of the cluster (derived from the integrated apparent magnitude and the distance modulus).

Constraint (*a*) is already satisfied, since it determines the value of the concentration parameter β_1 for the models. We were able to find a set of white-dwarf fractions x_i to satisfy constraints (*b*) and (*c*). Table 1 compares the numbers of stars in the first four mass classes (these correspond to the observed part of the published luminosity function) for the luminosity function and for the model, and Table 2 gives the detailed parameters for the final model. The two estimates of M/L_V described in (*c*) above differ by only 0.04, which is insignificant.

We now know the total number of non–white-dwarf stars in each mass class, so we can construct the luminosity function for the cluster as a whole. The extended Sandage luminosity function was used to define the distribution of stars *within* each mass class. The discontinuities at the boundaries of each mass class were smoothed by averaging to produce a continuous curve, while taking care that the number of stars in each mass class did not change. The resulting total luminosity function is shown in Figure 2, together with the extended Sandage function. The mass of the stars at the peak of the function is approximately 0.25 $M_\odot$. Figure 3 shows how well the model reproduces the observed surface brightness profile over five decades in surface brightness.

IV. DISCUSSION

There is some evidence (Oort and van Herk 1959; Woolf 1964) that the horizontal-branch stars of M3 are less centrally concentrated than the red giants,

TABLE 1

COMPARISON WITH SANDAGE LUMINOSITY FUNCTION FOR BRIGHT STARS WITHIN 8 ARCMIN OF CLUSTER CENTER

Mass Class	Fraction of Stars within $r/r_t = 0.2$	No. of Stars within $r/r_t = 0.2$ excluding White Dwarfs	No. of Stars as Given from Sandage Luminosity Function
1.....	0.89	5130	5100
2.....	0.86	9690	9680
3.....	0.81	10625	10565
4.....	0.75	20080	20075

TABLE 2

PARAMETERS OF CLUSTER MODEL

Mass Class	m_i ($M_\odot$)	β_i	μ_i	Percent of Total Mass	$\langle M_V \rangle$	Percent of Total V Light	Percent of Central V Light	Percent of Total White Dwarfs (by no.)	White Dwarf Percentage of Mass Class (by no.)
1	0.83	69.0	1.00	2.9	1.27	69.3	80.4	6.8	51.3
2	0.77	66.8	1.66	4.8	4.14	9.7	8.9	10.8	46.1
3	0.71	64.0	1.80	5.3	5.10	4.7	3.1	12.7	45.9
4	0.63	60.5	2.89	8.4	6.08	3.9	1.7	19.3	38.8
5	0.55	56.4	3.50	10.2	7.36	1.9	0.5	20.9	30.1
6	0.47	51.8	4.60	13.5	8.87	0.8	0.2	22.5	20.8
7	0.38	46.8	4.41	12.9	10.4	0.3	0.0	7.0	5.5
8	0.30	41.4	5.22	15.3	11.8	0.0	0.0	0.0	0.0
9	0.23	36.1	6.93	20.3	13.3	0.0	0.0	0.0	0.0
10	0.12	26.7	2.17	6.4	15.3	0.0	0.0	0.0	0.0
Horizontal branch					0.8	9.4	5.2		
White dwarfs					12.0	0.0	0.0		

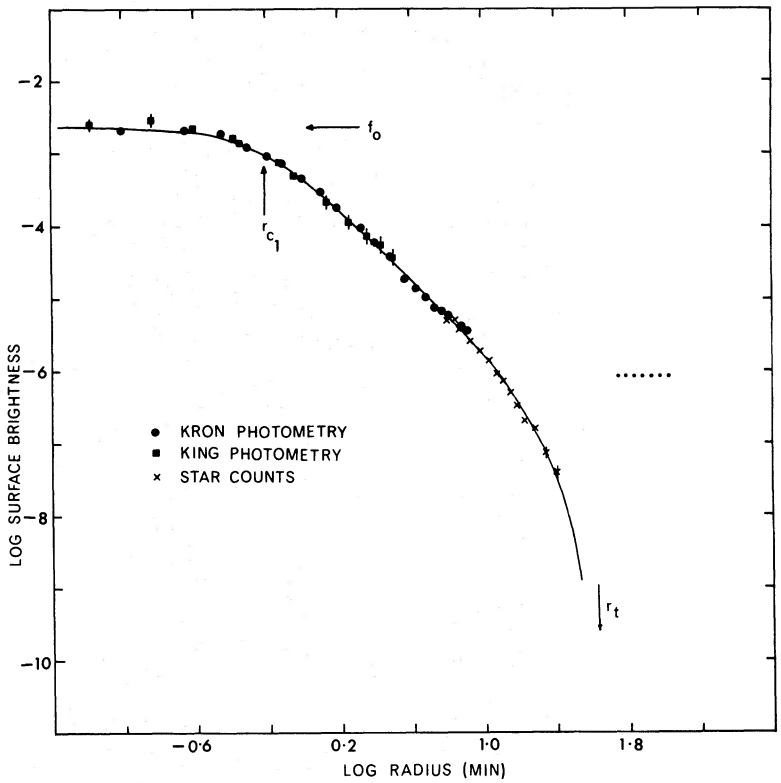

FIG. 3.—Comparison of the surface brightness profile of model C with the observed points. The central surface brightness f_0, the core radius of mass class 1, $r_{c,1}$, and the tidal radius r_t are indicated. The dotted line is the background level for the star counts.

indicating perhaps that the horizontal-branch stars have lost mass in post–red-giant evolution and have relaxed to the distribution characteristic of their new mass. So in constructing the theoretical profile of Figure 3, the horizontal-branch stars were assumed to be equally distributed between mass classes 3 and 4, giving a mean mass for these stars which is 80 percent of the red-giant mass. In an attempt to test this assumption, a second theoretical profile was constructed, this time assuming that the horizontal-branch stars were distributed in the same way as the giants. However, the difference between the two profiles was small and the fit to the observational data not significantly different. In constructing both these profiles, a mean M_V of 0.8 was assumed for the horizontal-branch stars, corresponding to a distance modulus of 14.83 (Sandage 1970) for the cluster.

Table 3 lists the parameters of M3 derived from the model. The uncertainty in the cluster mass arises because the model gives the mass of the cluster as $(4.01 \times 10^5)m_g$, where m_g is the mean mass of the stars of mass class 1. Mainly because of the uncertainty in the age of the cluster, the value of m_g is uncertain by about $\pm 0.04\ M_\odot$. We have not included any uncertainty in the cluster mass resulting from the extension of the Sandage luminosity function used, or indeed for any uncertainty in the Sandage luminosity function itself. However, the excellent agreement between the

TABLE 3

PARAMETERS OF M3

Mass of cluster M_{cl}	$(3.30 \pm 0.15) \times 10^5\ M_\odot$
Integrated apparent magnitude m_V	6.34
Distance modulus $(m - M)_{app,V}$	14.83
Mass to light ratio M/L_V	1.6 ± 0.2 (solar units)
Mean stellar mass	$0.33\ M_\odot$
Adopted mass of cluster giants	$0.83\ M_\odot$
Mean horizontal-branch star mass	$0.67\ M_\odot$
Adopted mean white-dwarf mass	$0.60\ M_\odot$
Core radius $r_{c,1}$	0.′60 or 1.6 pc
Tidal radius r_t	41′ or 110 pc
Central density d_0	$880\ M_\odot\ pc^{-3}$
Central escape velocity $(v_e)_0$	$18.4\ km\ s^{-1}$
Central line-of-sight velocity dispersion of giants $(\langle v_1^2 \rangle_{0,r})^{1/2}$	$3.7\ km\ s^{-1}$

model surface brightness profile and the observed profile and between the two estimates of M/L described in the previous section (constraint [c]) suggest that the results are not seriously in error.

As a check on the mass and tidal radius observed here, the limiting radius $r_{\rm lim}$ imposed on the cluster at its present position by the tidal galactic field was calculated. The limiting radius is given (King 1962, eq. 12) as:

$$r_{\rm lim} = R_G(M_{\rm cl}/3.5M_G)^{1/3},$$

where R_G is the present distance of the cluster from the galactic center and $M_G = 10^{11}\ M_\odot$ is the mass of the Galaxy. Then taking the distance between the Sun and the cluster as 9.2 kpc and assuming that the Sun is 10.0 kpc from the galactic center, we find that $R_G = 12.5$ kpc at the galactic latitude and longitude of the cluster. Then using $M_{\rm cl}$ from Table 3, we find that $r_{\rm lim} = 122$ pc, while the tidal radius is 110 pc. This agreement between the two figures is possible only if M3 is currently near perigalacticon. Using similar arguments and other data, Peterson (1974) gives the distance between the present position and the perigalacticon for M3 in the Schmidt (1965) model of the Galaxy as only 200 pc; we conclude that the cluster's mass and tidal radius as given in Table 3 are not inconsistent with its present position in the Galaxy.

The uncertainty in the M/L_V value for M3 given here reflects both the uncertainty in the mass and in the distance modulus of the cluster. The value, 1.6 in solar units, agrees well with the work of Illingworth (1973), who used the single mass models of King (1966*a*) and central velocity dispersions derived from coudé spectra of the integrated light to derive mass and M/L_V values for 10 centrally concentrated globular clusters. He finds M/L_V values ranging from 0.9 to 2.8, with a median value of 1.5.

Figure 4 shows the mass function of the cluster as derived from the model. There is no evidence for the deficiency in low-mass stars as has been suggested for globular clusters (Ostriker, Spitzer, and Chevalier 1972; Tayler and Wood 1975). It also suggests that the present mass function of this cluster, a Population II object formed at an early stage in the evolution of the Galaxy, conforms to the Salpeter initial mass function of Population I which has $dN = m^{-2.3}dm$. However, much significance should not be placed on this particular result, since the original extension of the luminosity function was based on the solar-neighborhood luminosity function from which the Salpeter "law" is derived, but there can be no doubt that M3 does contain large numbers of low-mass stars. The reason for this can perhaps be explained this way. The dependence of escape rate on stellar mass in a globular cluster is small (King 1966*c*); only those stars with masses much less than the average stellar mass escape significantly faster than stars of average mass. In our model of M3, the average mass is small (0.33 $M_\odot$), so only the very low-mass stars could be expected to be significantly depleted. This may explain the low relative total mass of mass class 10 in the model.

According to the model, M3 contains a total of 1.0×10^6 stars; more than half of them have masses below 0.5 $M_\odot$, 8.8 percent of them are white dwarfs, and 0.05 percent are horizontal-branch stars. It is interesting to note that the region $r/r_t \leq 0.2$, from which the Sandage luminosity function was derived, contains 54 percent of the total number of stars and 60 percent of the total mass, but 91 percent of the total V light! This clearly shows the degree of central concentration of the massive stars which contribute most of the light from the cluster. The effects of equipartition are also illustrated in Figure 5 which shows log (surface density of stars) against log (radius) for each mass class. The more massive stars are strongly concentrated toward the cluster center, while the low-mass stars are almost evenly distributed throughout the cluster. Figure 5 also illustrates the decrease in stellar density as the tidal radius is approached, the effect being similar for each mass class, since the tidal force of the Galaxy removes stars from the cluster independent of their mass.

Figure 6 shows the effects of equipartition on the surface density/number density and surface density/luminosity ratios with radius. A significant feature is the marked radial variation of the surface density-to-surface brightness ratio $\Sigma(r)/I(r)$, and in particular its low central value: $\Sigma(0)/I(0) = 0.4$ compared with the mean value of $M/L = 1.6$ for the whole cluster. Peterson and King (1975) have recently shown how important cluster parameters, such as the density, relaxation time, and escape velocity at the center of a cluster can be derived from $\Sigma(0)$, r_c, and the concentration parameter c. It appears now that the low central value of Σ/I is more appropriate for estimating $\Sigma(0)$ from the observed central surface brightness $I(0)$. We should, however, emphasize that although $M/L \approx$

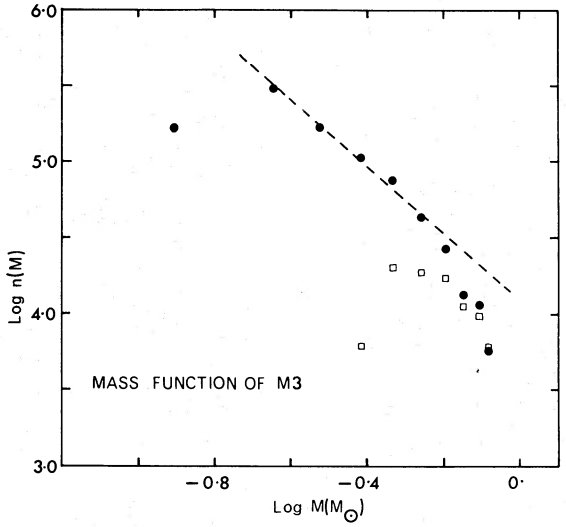

FIG. 4.—The mass function of M3. The logarithm of the number of stars in each mass class is plotted against the logarithm of the adopted stellar mass of the mass class. *Squares* give the number of white dwarfs in each mass class; *dots*, the number of non–white dwarf stars. The broken line has the slope of the Salpeter function.

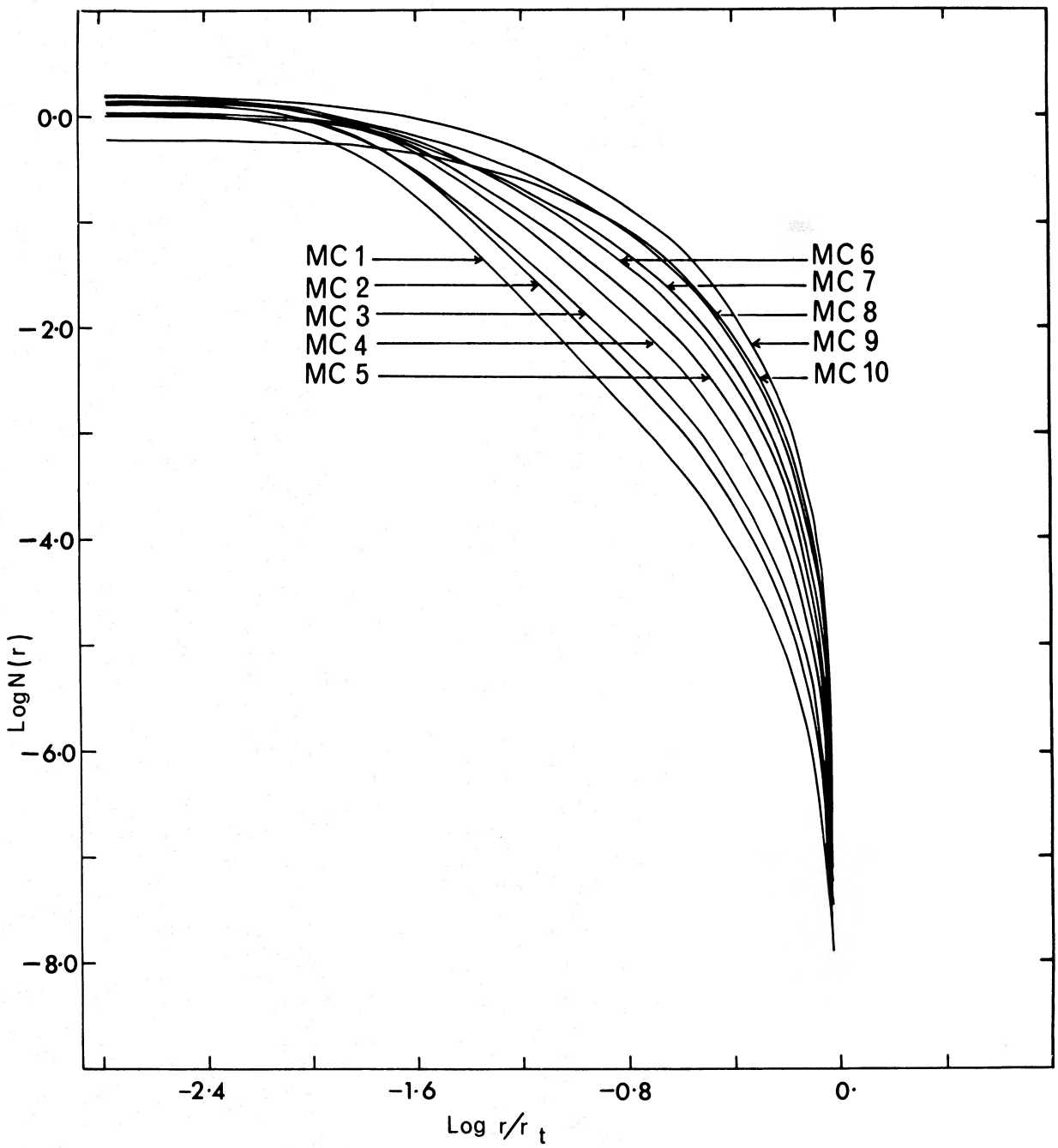

FIG. 5.—Distribution of stars of each mass class with radius. Ordinate is the logarithm of the surface density of stars of each mass class normalized so that the central surface density of mass class 1 is 1.0.

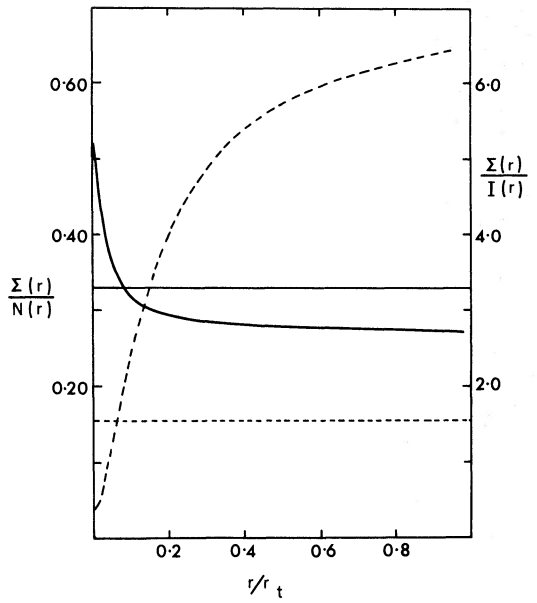

FIG. 6.—Variation of average stellar mass and mass-to-light ratio with radius. *Solid curve*, the ratio of surface density to surface number density $\Sigma(r)/N(r)$; *broken curve*, the ratio of surface density to visual surface brightness $\Sigma(r)/I(r)$. The straight lines represent the averages over the entire cluster.

1.6 seems to be a typical value for the mass-to-light ratio for a *whole* cluster, the value of $\Sigma(0)/I(0)$ will vary significantly from cluster to cluster, depending on the degree of central concentration of the cluster.

In conclusion, it appears that the globular cluster M3 can be well represented by a tidally limited model in which the stellar distribution is fully relaxed and not deficient in low-mass stars. Whether this conclusion applies to other clusters is a question that can only be answered by further study of these interesting objects.

The authors are very grateful to Drs. G. E. Kron and A. V. Hewitt for communicating their data on M3 in advance of publication, and to D. W. Carrick for advice in the early stages of program development. G. S. D. C. acknowledges the financial support of a Commonwealth Postgraduate Research Award. The calculations were performed on the Univac 1108 computer of the Australian National University.

REFERENCES

Copeland, H., Jensen, J. O., and Jørgensen, H. E. 1970, *Astr. and Ap.*, **5**, 12.
Greenstein, J. L., Neugebauer, G., and Becklin, E. E. 1970, *Ap. J.*, **161**, 519.
Harris, D. L., III. 1963, *Basic Astronomical Data*, ed. K. Aa. Strand (Chicago: University of Chicago Press), chap. 14, p. 263.
Harris, D. L., III., Strand, K. Aa., and Worley, C. E. 1963, *Basic Astronomical Data*, ed. K. Aa. Strand (Chicago: University of Chicago Press), chap 15, p. 273.
Iben, I. 1971, *Pub. A.S.P.*, **83**, 697.
Illingworth, G. D. 1973, unpublished Ph.D. thesis, Australian National University.
Johnson, H. L. 1966, *Ann. Rev. Astr. and Ap.*, **4**, 193.
King, I. R. 1962, *A.J.*, **67**, 471.
———. 1965, *A.J.*, **70**, 376.
———. 1966*a*, *ibid.*, **71**, 64.
———. 1966*b*, *ibid.*, p. 276.
———. 1966*c*, *The Theory of Orbits in the Solar System and Stellar Systems, IAU Symposium No. 25*, ed. G. Contopoulos (New York: Academic Press), p. 51.
King, I. R., Hedemann, E., Hodge, S. M., and White, R. E. 1968, *A.J.*, **73**, 456.
McCluskey, G. E., Jr., and Kondo, Y. 1972, *Ap. and Space Sci.*, **17**, 134.
Michie, R. W. 1963, *M.N.R.A.S.*, **125**, 127.
Oort, J. H., and van Herk, G. 1959, *Bull. Astr. Inst. Netherlands* **15**, 299.
Ostriker, J. P., Spitzer, L., and Chevalier, R. A. 1972, *Ap. J. (Letters)*, **176**, L51.
Peterson, C. J. 1974, *Ap. J. (Letters)*, **190**, L17.
Peterson, C. J., and King, I. R. 1975, *A.J.*, **80**, 427.
Prendergast, K. H., and Tomer, E. 1970, *A.J.*, **75**, 674.
Salpeter, E. E. 1955, *Ap. J.*, **121**, 161.
Sandage, A. 1954, *A.J.*, **59**, 162.
———. 1957, *Ap. J.*, **125**, 422.
———. 1970, *ibid.*, **162**, 841.
Schmidt, M. 1965, *Galactic Structure*, ed. M. Blaauw and M. Schmidt, (Chicago: University of Chicago Press), chap. 22, p. 513.
Shipman, H. L. 1972, *Ap. J.*, **177**, 723.
Simoda, M., and Iben, I. 1970, *Ap. J. Suppl.*, **22**, 81.
Tayler, R. J., and Wood, P. R. 1975, *M.N.R.A.S.*, **171**, 467.
Trimble, V., and Greenstein, J. L. 1972, *Ap. J.*, **177**, 441.
Vardya, M. S. 1970, *Ann. Rev. Astr. and Ap.*, **8**, 87.
Wickramasinghe, D. T., and Strittmatter, P. A. 1972, *M.N.R.A.S.*, **160**, 421.
Wielen, R. 1973, *Highlights of Astronomy*, **3**, 395.
Wilson C. P. 1975, *A.J.*, **80**, 175.
Woolf, N. J. 1964, *Ap. J.*, **139**, 1081.

G. S. DA COSTA and K. C. FREEMAN: Mount Stromlo and Siding Spring Observatory, Private Bag, Woden P.O., A.C.T., Australia, 2606